

536.423.1:532.595:621.18

Paper No. 170-11

Flow Instabilities in Boiling Channels*

Part 2 Geysering

By Mamoru OZAWA**, Shigeyasu NAKANISHI***, Seikan ISHIGAI†,

Yuhsuke MIZUTA†† and Hiroaki TARUI†††

An experimental study on geysering was carried out in an R-113 forced flow boiling system. The effects of flow rate, heat flux density, system pressure and heating condition on the threshold of geysering and on the period and amplitude of the differential pressure at the test section were studied. The mechanism of geysering was analyzed by using a simple model. The analytically predicted period and amplitude of oscillation agreed qualitatively with the experimental result and thus supported the validity of the model.

1. Introduction

Various types of flow instabilities⁽¹⁾ in a boiling two-phase flow system may cause severe operational and safety problems of the system. The preceding papers reported analytical and experimental investigations on the density wave oscillation^(2,3) and the pressure drop oscillation.⁽⁴⁾

This paper presents the result on geysering which is a nonlinear oscillation due to the liquid superheat and the violent boiling in a boiling channel.

Geysering is often observed in a vertical heated channel, in which there is little or no circulation and which opens into a vessel with a free liquid surface. Geysering is characterised by a rapid ejection of the liquid due to the violent boiling and the fall back of the liquid. It is desirable to avoid geysering with such adverse effects as the water hammer due to the fall back of the liquid.

Griffith⁽⁵⁾ has investigated geysering in a heated channel system with no circulation, and has reported that geysering is suppressed by limiting the free volume in the vessel and that the period of geysering is the order of 10 to 100 seconds. But there are no sufficient investigations on geysering in a heated channel system with circulation.

In this paper, the experimental results obtained by using the same boiling loop in the previous papers^(2,4) are presented and the effects of the operating parameters on the threshold condition of geysering, the period and the amplitude of the fluctuation of the pressure drop across the heated channel are investigated. A simple analysis on the

period of geysering and on the amplitude of the fluctuation of the pressure drop is made by modeling the temperature distribution along the channel and the processes of fall back and ejection of the liquid. This model is tested by comparing with the experimental results.

Notations

A_t	: cross sectional area of the heated tube
A_d	: cross sectional area of the drum
c_p	: specific heat of the liquid
c_d	: specific heat of the tube
D	: inner diameter of the heated tube
D_t	: outer diameter of the heated tube
g	: gravitational acceleration (9.8 m/s ²)
G	: mass flow rate
h_{fg}	: latent heat of vaporization
L_h	: heated length
L_r	: riser length
n	: polytropic exponent
P	: pressure
q	: heat flux density
Q	: power input
t	: time
T_{in}	: liquid temperature at the inlet of the heated section
T_s	: saturation temperature
$\Delta T_{sub} = T_s - T_{in}$	
w_{in}	: velocity at the inlet of the heated section
w_r	: rising speed of the liquid level due to the fall back of the liquid
x	: quality
z	: coordinate
α	: void fraction
ρ_f	: density of the saturated liquid
ρ_g	: density of the saturated vapor
$\rho_{fg} = \rho_f - \rho_g$	
ρ_t	: density of the tube

2. Experimental apparatus and experimental procedure

The experimental apparatus used in this study is the same one used in the previous papers^(2,4) except for a heated section. The heated section is a vertical SUS304 tube, 18.3mm I.D., 21.5 mm O.D., 3.0 m heated length and 3.0 m interval of two pressure

* Received 4th April, 1977.

** Research Associate, Faculty of Engineering, Osaka University, Suita.

*** Associate Professor, Faculty of Engineering, Osaka University, Suita.

† Professor, Faculty of Engineering, Osaka University, Suita.

†† Engineer, Prefectural Office, Fukui.

††† Engineer, Sumitomo Metal Industries Ltd., Amagasaki.

taps. It is heated directly by AC power, and the heat flux density is uniform. To permit visual observation of the flow, a sight glass tube is installed in the riser section of 0.6 m length downstream of the heated section. The pressure drops at the Venturi flowmeter and the heated section are measured by D.P. cells and strain amplifiers and are recorded by a pen recorder. The tube wall temperatures are measured by 6 C-A thermocouples of 0.3 mm diameter. In this experiment, the bypass valve V_5 , shown in Fig.1 in the previous paper,⁽⁴⁾ is closed and the surge tank is isolated from the system.

The experiments are conducted in such a way that the data of the threshold of geysering can be plotted on the power vs. inlet velocity plane. The system pressure, the flow rate and the inlet temperature of the liquid are brought to a predetermined steady state, and then the power input is increased in small steps until geysering occurs.

The experiments are divided into 5 series, as shown in Table 1, according to the combination of the heated length L_h and the riser length L_r illustrated in Fig.1.

Table 1 Heating condition

	L_h m	L_r m
a	3.0	0.6
b	2.15	0.6
c	1.0	0.6
d	2.15	1.45
e	1.0	2.6

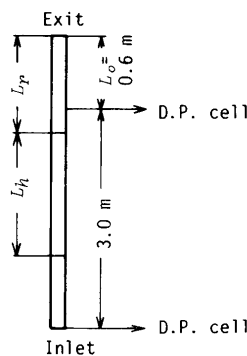


Fig. 1 Test section

The experimental range is as follows:
 the system pressure 0.101-0.196 MPa
 the inlet velocity 0.0056-0.0236 m/s
 the inlet subcooling 10-45 K

In this experimental range, the friction pressure drop and the acceleration pressure drop are very small compared with the gravitational pressure drop. According to the analysis by Griffith⁽⁵⁾ when the system has a larger free volume than that given by Eq. (1)

$$V_d = \frac{nP}{(1/A_i - 1/A_d)\rho_f g} \dots\dots\dots(1)$$

geysering can be observed in a system with no circulation. In this experiment, the free volume in the drum is about 0.1 m³ which is much bigger than the value 0.0025 m³ obtained from Eq.(1) for the system pressure 0.101 MPa.

3. Experimental results

3.1 General feature of geysering

The typical traces of the pressure drop at the Venturi flowmeter (corresponding to the inlet flow rate) and the pressure drop across the heated section are shown in Fig.2. At the state (A), a small fluctuation in the pressure drop across the heated section is observed, but no bubble is observed at the sight section. This small fluctuation is considered to be caused by the normal sub-cooled boiling in the heated channel. When the power input increases beyond a certain limit, a large fluctuation in the pressure drop across the heated section occurs (B). At the sight section, it is observed that this oscillation has three processes, i.e. a single phase flow of the liquid (the 1st process), a rapid ejection of the vapor-liquid mixture (the 2nd process) and a fall back of the liquid from the drum (the 3rd process). The oscillation characterised by these three processes is referred to as geysering. The amplitude and the period of this oscillation increase with an increase in the power input (C). Three periods denoted by τ_1 , τ_2 and τ_3 as seen in the diagram represent these three processes respectively. The amplitude of the fluctuation of the pressure drop across the heated section is very large, whereas no fluctuation is observed in the inlet flow rate. This fact indicates that the elements of the boiling loop concerned with this oscillation are the heated section, the riser section and the drum. As the power input increases

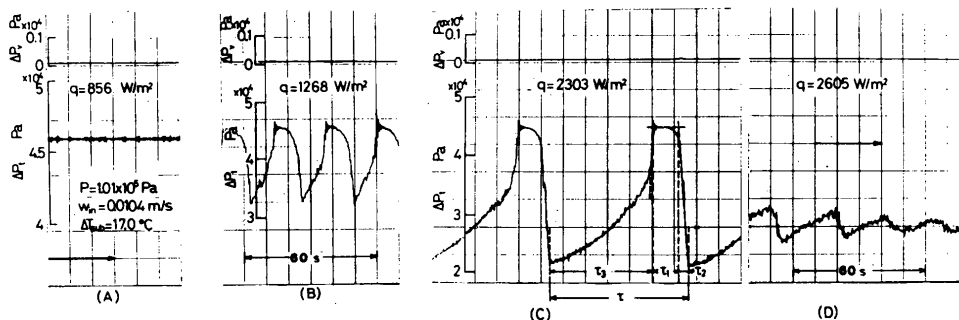


Fig. 2 Typical trace of the oscillation

beyond a certain limit, geysering subsides gradually to a stable state with a small fluctuation due to the normal boiling noise (D). When the riser length is 0.6 m a fluctuation in the pressure drop ΔP_f due to the periodic transition from the bubbly flow to the slug flow is observed. This fluctuation is not considered geysering in this paper, because the three characteristic processes mentioned above are not involved. Geysering can be observed not only in the forced circulation experiments but also in the natural circulation experiments.

3.2 Threshold of geysering

The threshold of geysering for the heating condition (a) is shown in Fig.3 on the power input Q vs. inlet velocity w_{in} plane. Geysering is observed in the experiments represented by solid circles. The threshold condition is represented by the solid line. The range of power inputs, in which geysering is observed, converges with an increase in the inlet velocity, and geysering cannot be observed when the inlet velocity is beyond 0.02 m/s. In cases of the other operating conditions, there are some limitations in the power input and the inlet velocity for the occurrence of geysering. When the vapor-liquid mixture is rapidly ejected by the violent boiling, the static pressure in the channel decreases to a value nearly equal to the drum pressure. The boiling region must therefore extend to the position where the liquid temperature is equal to the saturation temperature for the drum pressure. Since the inlet velocity does not fluctuate during geysering, as shown in Fig.2, and the wall temperature fluctuations are not observed in the subcooled liquid region, where the liquid enthalpy is below the saturated liquid enthalpy

for the drum pressure, the subcooled liquid region has no effect on geysering. Consequently, the main parameters concerned with geysering are the power input, the boiling length L_e and the inlet velocity. In this paper, the threshold of geysering is presented by using two parameters, i.e. the heat flux density q and the residence time in the boiling region τ_e , which are defined as follows:

$$q = \frac{Q}{\pi D L_e} \dots\dots\dots(2)$$

$$\tau_e = \frac{L_e}{w_{in}} \dots\dots\dots(3)$$

where the boiling length is given by

$$L_e = L_h - \frac{G c_p \Delta T_{sub}}{q \pi D} \dots\dots\dots(4)$$

Figure 4 shows the threshold of geysering in the case of the heating condition (a). The threshold condition is represented by one curve in spite of various values of the inlet subcooling. In the region $\tau_e \leq 100$ s, geysering does not occur, and the maximum heat flux density for the occurrence of geysering is about 2300 W/m², while the minimum heat flux density decreases with an increase in τ_e . Figure 5 shows the experimental results for the heating condition (b) and (d). In these cases geysering is observed in the range of $\tau_e \geq 60$ s, and the maximum value of q for the occurrence of geysering is higher than for the heating condition (a). The figure also shows that a longer riser has a wider geysering range. Figure 6 shows the effect of the system pressure on the threshold of geysering. The solid line represents the threshold condition for $P=0.196$ MPa, and the broken line for $P=0.108$ MPa. This shows that the pressure is a damping factor for geysering.

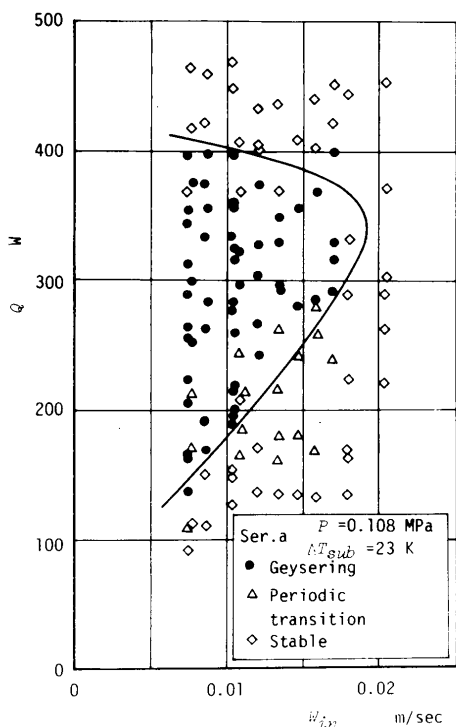


Fig. 3 Threshold of geysering

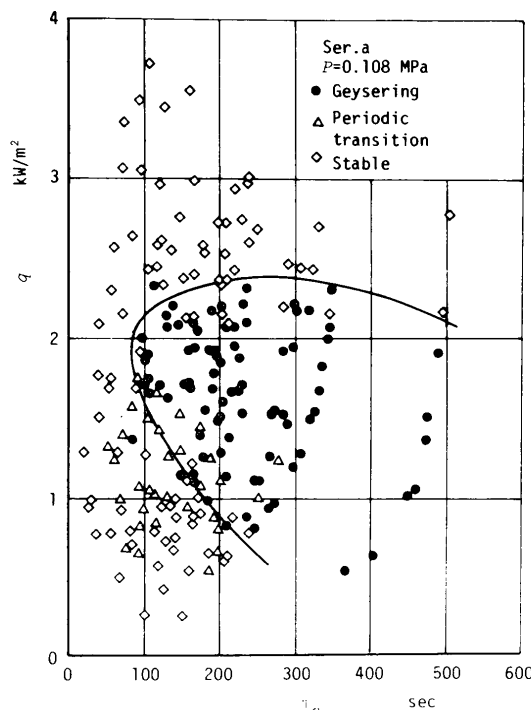


Fig. 4 Threshold of geysering

In the case of the heating condition (c), geysering cannot be observed and only a periodic transition from the bubbly flow to the slug flow and then back to the bubbly flow is observed. On the contrary, in the case of the heating condition (e) the geysering region is wider than for the heating conditions (a), (b) and (d), and the maximum heat flux density for geysering amounts to 8100 W/m^2 . This fact shows that the riser length is a destabilizing factor for geysering.

3.3 Geysering period

In Fig.7, the geysering period τ is plotted against the heat flux density q . The period increases with the heat flux density and decreases with the inlet velocity. In cases of the heating conditions (b) and (d) as shown in Figs.8 and 9, the geysering period has the same tendency as under the heating condition (a).

3.4 Amplitude of geysering

The amplitude of the fluctuation in the pressure drop across the heated section also depends on the heat flux density, the inlet velocity and the heating condition. In this paper the difference between the maximum and the minimum of the pressure drop across the heated section is referred to as the amplitude δP of geysering. The amplitudes of geysering for the heating condition (a), (b) and (d) are shown against the heat flux density q and the inlet velocity w_{in} . At any heating condition, the amplitude increases with an increase in the heat flux density and a decrease in the inlet velocity. By comparing Fig.10 with Fig.11, it is seen that the amplitude increases with an increase in the heated length. And from the comparison between Fig.11 and Fig.12, it is seen that the amplitude increases with an increase

in the riser length.

The reason for the effects of these parameters on the amplitude of geysering is estimated as follows: The boiling length L_e increases with an increase in the heat flux density, and with a decrease in the inlet velocity. When the boiling length increases, the size of the vapor slug generated during the violent boiling increases, and then the mass of the liquid ejected into the drum increases. This results in an increase in the amplitude of geysering. With an increase in the riser length, the mass of the liquid ejected into the drum also increases, and this causes an increase in the amplitude.

4. Analysis

4.1 Mechanism of Geysering

Griffith⁽⁵⁾ has shown that a geysering is caused by one of the two mechanisms, i.e., a violent boiling due to the liquid superheat, or a self evaporation due to the drop in the pressure. Geysering in a system without circulation is certainly well explained by these two mechanisms. But they do not sufficiently explain the sustained geysering in a system with circulation. It is necessary that the heated channel be repeatedly filled with the liquid for the occurrence of a sustained geysering in the system with circulation. If the bubbles generated in the channel are quickly ejected by the flow and a large vapor slug is not generated, there can be no geysering. This is the case of the heating condition (c). In conclusion, for sufficient understanding of the sustained geysering in the system with circulation, it is necessary to take into account the processes of the fall back of the liquid from the drum, the bubble growth and the ejection of the bubble. The main purpose of this analysis is to correlate the data of the geysering period and the amplitude of geysering. This analysis concerns only the case that a vapor slug can be generated in the channel by one of two mechanisms described by Griffith⁽⁵⁾. Therefore the processes of the bubble growth and the ejection of

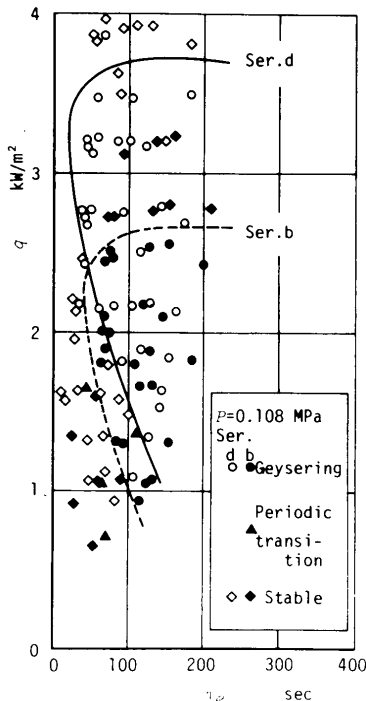


Fig. 5 Threshold of geysering

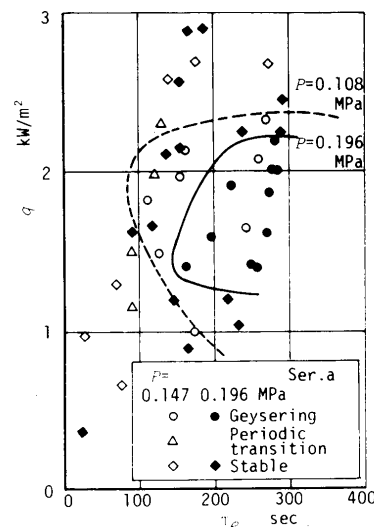


Fig. 6 Threshold of geysering

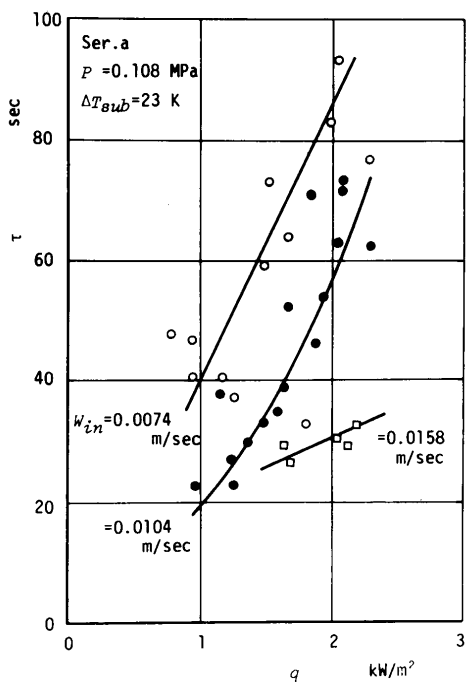


Fig. 7 Period of geysering

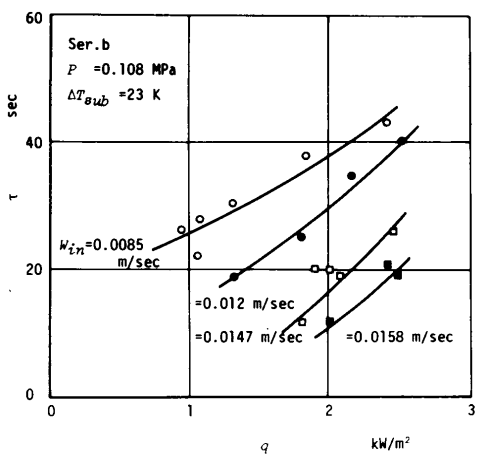


Fig. 8 Period of geysering

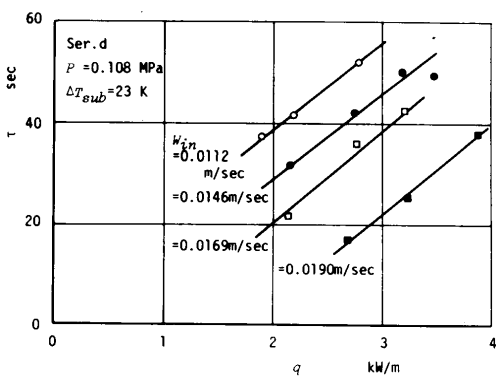


Fig. 9 Period of geysering

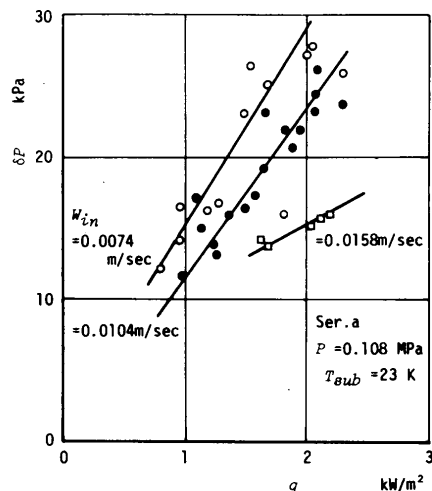


Fig. 10 Amplitude of geysering

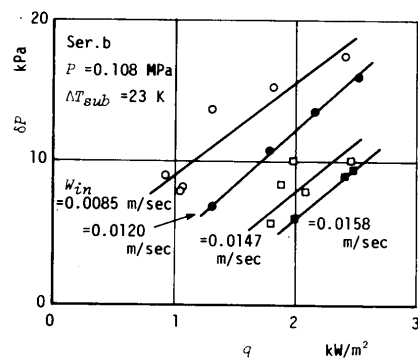


Fig. 11 Amplitude of geysering

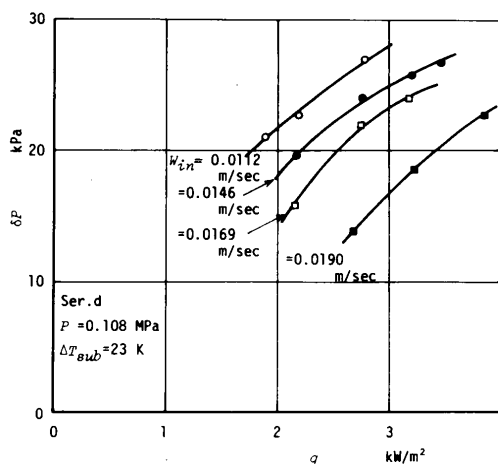


Fig. 12 Amplitude of geysering

the bubble are not taken into account in this analysis.

4.2 Geysering period

Figure 13 shows a model of the channel during geysering. The coordinate along the channel z is shown in the opposite direction to the steady flow, and $z=0$ at the inlet of the drum. When some of the liquid is ejected by the vapor slug generated due to a violent boiling in the channel (Fig.13-1), the static pressure in the channel decreases, and this results in further growth of the vapor slug (Fig.13-2). It follows that the pressure in the channel becomes nearly equal to the drum pressure (Fig.13-3), and the boiling region extends to the position $z_g = L_e + L_r$ where the liquid enthalpy is equal to the saturated liquid enthalpy for the drum pressure. Then the fluid in between $z=0$ and $z=z_g$ is at the saturation temperature T_s for the drum pressure. When the violent boiling finishes, the liquid in between $z=0$ and $z=z_g$ falls down to the bottom and the liquid level in the channel is at the position z_v . In this experimental range, the friction and the acceleration terms of the pressure drop are too small compared with the gravitational term, so the pressure drop across the heated section can be considered to be equal to the gravitational pressure drop. The density of the vapor is so small compared with the density of the liquid in this experimental range, for example $\rho_g/\rho_f = 0.00518$ at $P = 0.108$ MPa, that the density of the vapor is ignored. The channel length z_v occupied by the vapor just after the ejection of the vapor slug (Fig.13-4) is expressed by

$$z_v = \delta P / (\rho_f g) + L_o \quad \dots\dots\dots(5)$$

where L_o is the riser length which is not involved in the interval of the pressure taps (see Fig.1) and is 0.6 m.

In order to prepare a mathematical representation of the fluid temperature distribution along the channel and the behavior of the liquid level in the channel, it is necessary to make the following assumptions:

- (1) The liquid superheat can be ignored.
- (2) The liquid which falls back from the drum is at the saturation temperature for the drum pressure.
- (3) As the heated channel has a thin tube wall, the temperature of the tube wall is equal to the fluid temperature.

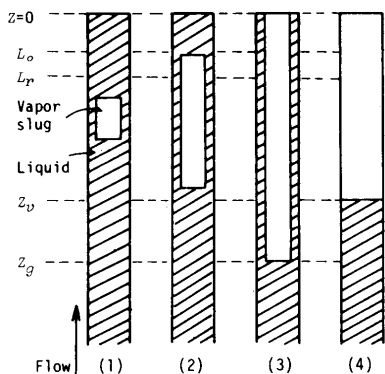


Fig.13 Model of the 1st process of geysering

(4) The rising speed of the liquid level in the channel due to the fall back from the drum is constant and is expressed as

$$w_r = z_v / \tau_3' - w_{in} \quad \dots\dots\dots(6)$$

Figure 14 shows the models of the temperature distribution along the channel (A) and the rising process of the liquid level (B). The figures (A-1) and (B-1) illustrate the final state of the violent boiling and correspond to the state shown in Fig.13-4. The liquid level in the channel rises due to the fall back from the drum and the inflow from the pump. During this process, the liquid in between z_v and z_g at the states (A-1) and (B-1) is heated and the temperature rises uniformly from T_s to T_2 as shown in (A-2). On the other hand, the temperature rise of the liquid, which enters the channel during the period between (B-1) and (B-2) due to the fall back and the inflow, depends on the heating period and is different at each position. Thus the temperature distribution along the channel forms a trapezoid. When the liquid level reaches the upper end of the heated section (B-3), the temperature distribution is similar to that at the state (A-2). When the liquid level reaches the top of the riser section, the distribution is in the shape of the state (A-4). In (A-4), the temperature distribution at the riser section differs from that at the heated section, because the riser section is not heated. At the state (A-5) the liquid temperature at a certain position in the channel reaches the saturation temperature for the static pressure at the same position. This corresponds to the state at the period $(\tau_1' + \tau_3')$ after the violent boiling. The liquid in between z_v and z_g just after violent boiling reaches the region in between $z_v - (\tau_1' + \tau_3') w_{in}$ and $z_g - (\tau_1' + \tau_3') w_{in}$, where the liquid temperature is T_s' and is given by the following equation:

$$T_s' = T_s + \frac{\pi D q (\tau_1' + \tau_3')}{A_i \rho_f c_p (1 + R)} \quad \dots\dots\dots(7)$$

where the notation R is the heat capacity ratio between the tube wall and the liquid, and is given by

$$R = \frac{\rho_w c_w (D_i^2 - D^2)}{\rho_f c_p D^2} \quad \dots\dots\dots(8)$$

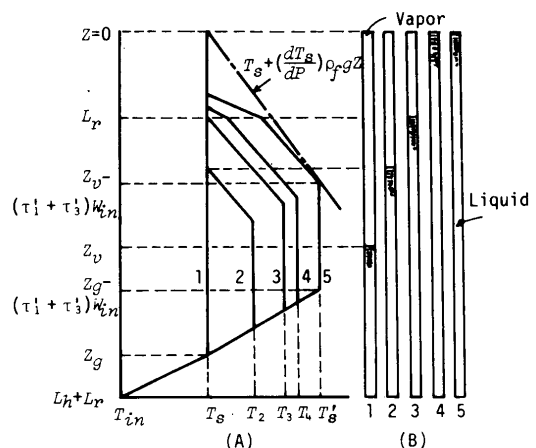


Fig.14 Temperature distribution and rising process of the liquid level

At the state (A-5), the liquid temperature at the position $z = z_v - (\tau_1' + \tau_3')w_{ln}$ coincides with the saturation temperature given by $T_s + (dT_s/dP)\rho_f g z$ and the boiling initiates at this point. Then the state in the channel returns to the state (A-1) and (B-1) through the process shown in Fig.13. At the state shown in (A-5),

$$T_s + \frac{\pi D q (\tau_1' + \tau_3')}{A_i \rho_f c_p (1+R)} = T_s + \left(\frac{dT_s}{dP} \right) \rho_f g (z_v - (\tau_1' + \tau_3')w_{ln}) \dots (9)$$

Substitution of Eq. (6) into Eq. (9) gives

$$\frac{\tau_1'}{\tau_3'} = \frac{(dT_s/dP)w_{ln}\rho_f g - (\pi D q / A_i \rho_f c_p (1+R))}{(dT_s/dP)w_{ln}\rho_f g + (\pi D q / A_i \rho_f c_p (1+R))} \dots (10)$$

For the condition $\tau_1'/\tau_3' \geq 0$, the heat flux density must satisfy the inequality

$$q \leq q_c \dots (11)$$

where

$$q_c = \frac{A_i}{\pi D} \left(\frac{dT_s}{dP} \right) \rho_f^2 g w_{ln} c_p (1+R) \dots (12)$$

Equation (10) represents the ratio between the time periods of the 1st process and the 3rd process, and it can be applied in the range given by Eq. (11). Thus Eq. (12) gives the maximum heat flux density for the occurrence of geysering. The periods τ_1' and τ_3' defined in the range between $z=0$ and $z=L_p+L_y$ do not exactly coincide with the periods τ_1 and τ_3 defined in the interval of two pressure taps. But the periods τ_1' and τ_3' are approximately equal to the periods τ_1 and τ_3 , because the residence time of the liquid level in the interval of $z=0 \sim L_o$ is very short compared with the period τ_1 and τ_3 in the actual experiments.

As the rising speeds of the liquid due to the fall back of the liquid w_{ln} obtained from the experiments and Eq. (6) distribute widely in the range of 0.02~0.1 m/s, the speed w_{ln} is chosen as an operating parameter for the correlation.

In Figs.15, 16 and 17 the ratio obtained from the experimental results is shown against the ratio obtained from Eq. (10) for the heating conditions (a), (b) and (d) respectively. The best correlation is obtained by the operating parameter $w_{ln}=0.05$ m/s for the heating condition (a), $w_{ln}=0.07$ m/s for the heating condition (b) and $w_{ln}=0.09$ m/s for the heating condition (d).

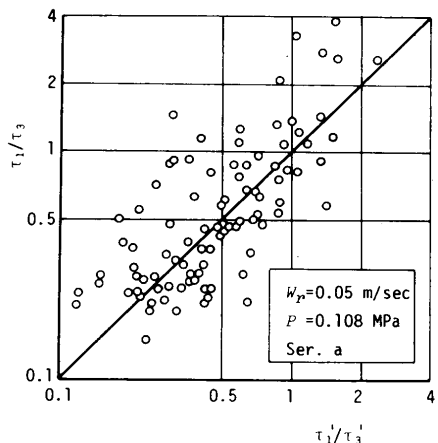


Fig. 15 Correlation of τ_1/τ_3

The maximum heat flux density obtained by Eq. (12) is 2550 W/m² for the heating condition (a), 3570 W/m² for the heating condition (b) and 4580 W/m² for the heating condition (d). The calculated maximum heat flux density is about 10 % higher than that of the experimental result for the heating condition (a). Two other values for the heating conditions (b) and (d) are 40 % and 25 % higher than the experimental results respectively. The effects of the heating length and the riser length on the maximum heat flux density coincide with the experimental results. In spite of the simplicity of this analysis using the model shown in Fig.14, the calculated results show rather good agreement with the experiment. As the process of the generation of the vapor slug is not taken into account in this analysis, the maximum values of the inlet velocity or the minimum values of the heat flux density for the occurrence of geysering can not be obtained.

4.3 Amplitude of geysering

It is necessary to know the temperature distribution along the channel just before the violent boiling in order to calculate the amplitude of geysering. As it is difficult to know the absolute values of τ_1' and τ_3' , the temperature distribution shown in Fig.14 is not available. In this paper, the temperatures of the liquid and the tube wall between $z=L_p$ and $z=z_g$ just before the violent boiling are assumed to be equal to

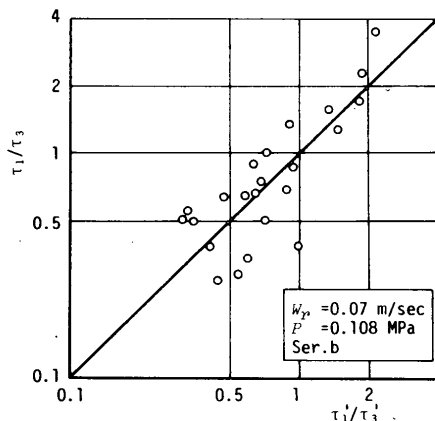


Fig. 16 Correlation of τ_1/τ_3

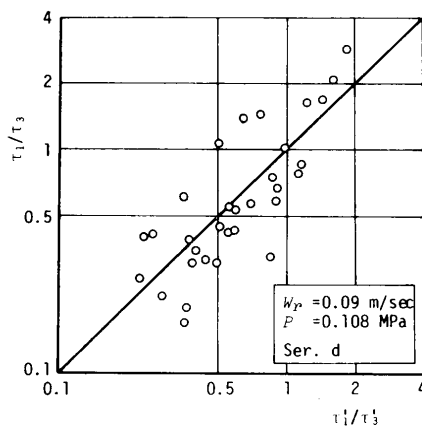


Fig. 17 Correlation of τ_1/τ_3

the saturation temperature T_{sr} for the static pressure at the exit of the heated section, i.e. $z = L_{gr}$. According to the process shown in Fig.13, the heat $(T_{sr} - T_g)c_p A t \times (z_g - L_{gr})\rho_f(1+R)$ is supplied for the vaporization of the liquid in the channel during the violent boiling. Then the quality between $z=0$ and $z=z_g$ is

$$\alpha = \frac{(T_{sr} - T_g)c_p(1+R)}{h_{fg}} \quad (13)$$

and the void fraction under the assumption that the slip ratio is unity is given by

$$\alpha = \frac{\rho_f z}{\rho_g + \rho_f z} \quad (14)$$

The amplitude of geysering is given by

$$\delta P = \rho_f g z_g \alpha \quad (15)$$

In this experiment, the tube length from $z=0$ to $z=L_o$ is not involved in the interval of two pressure taps. By assuming that the liquid in the channel just after the violent boiling falls down to the bottom as is shown in Fig.13-4, the amplitude of geysering is given by

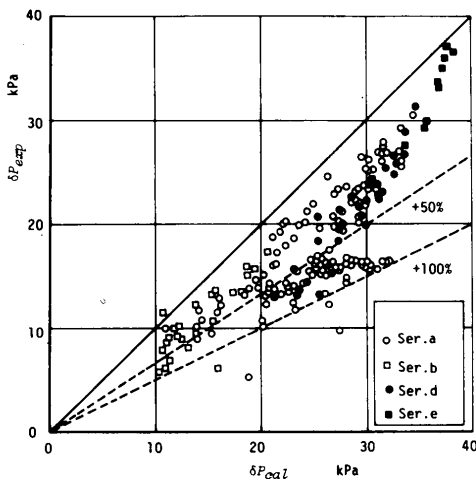


Fig.18 Amplitude of geysering (with heat capacity of the tube wall)

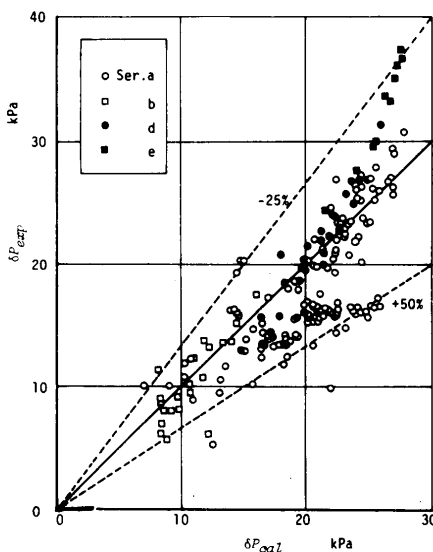


Fig.19 Amplitude of geysering (without heat capacity of the tube wall)

$$\delta P = \rho_f g(z_g \alpha - L_o) \quad (16)$$

In this model shown in Fig.13, the state of the minimum pressure drop is the state (3), but the transition from the state (3) to the state (4) is so fast that the pressure drop is considered to be minimum at the state (4).

Figure 18 shows the comparison between the experimental results δP_{exp} and the calculated results δP_{cal} . The calculated values are about 50 % larger than the experimental ones. The violent boiling takes place very quickly, so the heat capacity of the tube wall may not contribute to the amplitude of geysering. The calculated results of δP for the cases that the heat capacity of the tube wall is neglected, i.e. $R=0$ are compared with the experimental results in Fig. 19. The calculated results show rather good agreement with the experimental ones. In this experiment a model without heat capacity of the tube wall gives better correlation than one with the heat capacity of the tube wall, but it is found that the model represents the principal mechanism of the violent boiling.

Griffith⁽⁵⁾ shows that geysering may be observed in the systems of which the working fluids are water, methanol and R-11 similar to R-113, and that the experimental results in these systems can be correlated in the same manner as in his paper. This shows the availability of the model presented in our paper for other fluid systems as well.

5. Conclusions

The conclusions of this investigation are summarized as follows:

- (1) The inlet velocity and the system pressure affect geysering as a stabilizing factor, while the riser length affects as a destabilizing factor.
- (2) The geysering period increases with an increase in the heat flux density and a decrease in the inlet velocity.
- (3) The amplitude of geysering increases with an increase in the heat flux density and the riser length, and a decrease in the inlet velocity.
- (4) The calculated results of the ratio of the time periods τ_1' / τ_3' and the maximum heat flux density q_c' agree well with the experimental results.
- (5) The amplitudes of geysering obtained by Eq.(16) agree well with the experimental results.
- (6) The model in this paper represents the principal mechanism of geysering.

References

- 1) Bouré, J.A., et al., ASME Paper 71-HT-42 (1971), 1.
- 2) Nakanishi, S., et al., Theoretical and Applied Mechanics, Vol.26 (1978), 421.
- 3) Nakanishi, S., et al., Technology Reports of the Osaka Univ., Vol.28, No.1421 (1978), 243.
- 4) Nakanishi, S., et al., Bulletin of the JSME, Vol.22 No.170 (1979), 1113.
- 5) Griffith, P., ASME Paper 62-HT-39 (1962), 1.